

# COMPUTER ANALYSIS OF HOLO-INTERFEROGRAMS

by

Donald R. Matthys

Physics Department  
Marquette University  
Milwaukee, Wisconsin 53233

John A. Gilbert

Department of Mechanical Engineering  
University of Alabama in Huntsville  
Huntsville, Alabama 35899

T. Dixon Dudderar

AT&T Bell Laboratories  
Murray Hill, New Jersey 07974

## ABSTRACT

A systematic method for measuring surface deformation is developed which includes the use of real-time holographic fiber optic recording, the incorporation of a carrier pattern to achieve fringe linearization, image digitization, and automated computer analysis. This method has been tested at various levels of complexity; first by studying the deflection of a centrally loaded disk, then by applying it to study an hermetically sealed electronic package, and finally to the measurement of deformations in a complex printed wiring board with several surface mounted ceramic chip carriers.

## Introduction

Although interferometry is sometimes said to be one of the most significant applications of holography, it has not yet found widespread practical application. The major factor inhibiting full exploitation of the technique is the difficulty of getting quantitative results from holographic interferograms. Furthermore, the interferogram does not contain sufficient information to determine the sign of the surface displacement component being measured. However, the real root of the problem is that in many practical cases the interference patterns obtained are frequently so complex that even if the sign of the displacements were known, a skilled analyst could obtain quantitative results only with great difficulty. Therefore, if holography is to be commonly used as a measurement tool, some method of simplifying the analysis of interferograms must be developed. This simplification can be attained through image processing and computer analysis.

Early efforts to use digital methods in the study of holo-interferograms were limited to linear fringe distributions associated with simple translations or nearly uniform deformations [1-3]. Analysis of more complex displacements required the introduction of carrier fringes. This procedure was suggested by several investigators [4-6], and has been used by the authors for semi-automatic analysis of deflection (out-of-plane displacement) [7].

Applications in the electronics area were chosen to evaluate the potential for completely automating the measurement of displacement in more practical situations. Initial efforts were directed toward measuring surface deflections induced by environmental factors (including thermal and mechanical effects) on the surface of a hermetically sealed package used to house microelectronic components. This study demonstrated that a high level of automation can be achieved by using a photoelectronic-numerical system for analysis of real-time holographic interferograms. At the same time, problems resulting from boundary effects became evident, indicating the need for either more sophisticated numerical algorithms and/or for operator intervention.

Current efforts are being directed towards the application of this technique to measuring thermally induced surface displacements in printed circuit modules. These deformations impact seriously on the mechanical reliability of solder joints used to affix surface mounted components. In general the analysis is complicated by the presence of large numbers of surface mounted electronic components. These often cause rapid fluctuations in surface reflectivity which in turn produce abrupt changes in the intensity of the digitized image.

Results of this study show that the current approach can be used for measuring deflections in simple structures, but that refinements must be made if it is to be applied successfully to the analysis of the complex thermally induced deformations which occur in printed wiring boards.

## Theory and Background

Most holo-interferometric fringe patterns obtained in practical applications are too complex to be amenable to automated analysis. Therefore a carrier fringe pattern must be used to achieve fringe linearizations [4-7]. This technique involves superimposing a known linear phase shift on the phase shift distribution caused by surface deformation to produce a monotonically changing phase shift distribution across the interferogram. In this way, the complex fringes of the original interferogram are reduced to "nearly straight" fringes on which the deformation is superimposed as a modulation. Such fringes can be easily read in by a machine vision system. When the carrier fringes are later subtracted, the original information about the deformation is retrieved. In addition, the known phase characteristics of the carrier allow unambiguous determination of the sign of the displacement vector.

By proper choice of the illuminating and viewing directions, the sensitivity vector along which displacement is projected can be aligned normal to the surface under study thereby allowing out-of-plane displacement or deflection to be measured. However, measuring in-plane motion requires that the sensitivity vector be tangent to the surface. This in turn either (1) illuminating the object with a single source and viewing the object from two different locations, or (2) illuminating the object from two directions and viewing from a fixed direction. The latter approach can be easily implemented with a fiber optic system.

The use of single mode optical fibers for object and reference beam illuminators greatly simplifies the required experimental set-up for conventional holographic and holo-interferometric applications [8]. When coupled with so-called "instant" holographic recording systems, optical fibers provide a powerful new tool for optical measurement [9].

A holo-interferometric fringe pattern can be related to the deformation of the surface by the simple vector expression,

$$n\lambda = \bar{g} \cdot \bar{d} \quad 1$$

where  $n$  is the fringe order number,  $\lambda$  is the wavelength of coherent light used to record and reconstruct the hologram,  $\bar{g}$  is the sensitivity vector ( $\bar{e}_2 - \bar{e}_1$ ) where  $\bar{e}_1$  and  $\bar{e}_2$  are unit vectors in the illumination and observation directions respectively, and  $\bar{d}$  is the displacement vector at the point of observation on the surface of the sample. If a relatively flat surface is intentionally oriented normal to the angle bisector of  $\bar{e}_1$  and  $\bar{e}_2$ , the interferometer senses only the out-of-plane displacement component,  $W$ , and Equation (1) becomes,

$$n\lambda = 2W \cos \beta \quad 2$$



where  $2\theta$  is the angle between the propagation vectors in the directions of illumination and observation. A carrier pattern can be superimposed on this deformation to allow the fringe pattern to be sufficiently simplified for digital recording. Equation (2) characterizes the deflection when the carrier pattern is recorded separately and numerically subtracted from the superimposed deformation.

If the object is illuminated by two beams oriented symmetrically with respect to the surface normal (say each at an angle  $\alpha$ ), two holo-interferometric fringe patterns result. These are referred to as component patterns. The fringe orders can be numerically subtracted or the component patterns can be optically superimposed to produce a moire [10,11]. This superposition is characterized by the equation,

$$n\lambda = 2U \sin \alpha \quad 3$$

where  $n$  is the difference between the fringe order numbers in the component patterns,  $\lambda$  is the wavelength used to record and reconstruct the holo-interferograms, and  $U$  is the displacement component measured in the plane formed by the propagation vectors from the two sources and oriented perpendicular to their angle bisector. The same carrier pattern can be superimposed on each deformation pattern to facilitate digitization (or, for that matter, optical superposition). The effect of the common carrier vanishes when the patterns are subtracted numerically. Thus, the same basic approach used to record deflection is applicable for the measurement of in-plane displacement. The aim of this research program is to apply this procedure to problems of variable complexity and in particular to apply it to the study of thermal deformations in printed circuit modules.

The surfaces best suited to automated analysis are reasonably well behaved, relatively flat, and of nearly uniform reflectance. In most real problems the surfaces of interest move in a very complex manner, have irregular surface contours, and exhibit non-uniform reflectance. As described below, a printed wiring board with its surface mounted components displays all of these characteristics, presenting a formidable challenge to any automated system for holographically mapping surface deformation.

Micro-electronic modules with leadless surface mounted components may experience significant thermally induced warping and deformation during manufacture and subsequent service. Such behavior may impose severe loadings on the solder interconnections between the components and the mounting board which can result in rapid fatigue and premature failure. These deformations usually arise because of differences in the thermal-mechanical responses of the surface mounted components and the printed wiring board.

One approach to studying these has been to compare the thermal mechanical responses of different prototype designs by making whole-field deformation measurements using holo-interferometry, and various reports of earlier successful applications of this technique have been published elsewhere by some of the authors [12-15].

Figure 1, for example, shows a typical thermally loaded module with the resulting holo-interferometric fringe pattern as recorded using an optical configuration similar to that described in the following section.

## Feasibility Studies

In prior related research, the authors established the basic functionality of an automated holographic recording and analysis system by using it to study the problem of a centrally loaded disk. Figure 2 shows the isometric plot of the surface deflection of the disk obtained by a completely automated process [7]. In this case, the edge of the specimen was fixed, which simplified the identification of absolute fringe orders.

The next stage in developing this process was to apply it to a component with less restraint on its boundaries. A package used to house microelectronic circuit cards was used for this step. Its flat surface was positioned in the set-up shown in Figure 3 so that the out-of-plane displacement could be measured [using Equation (1)] with a fringe sensitivity of 0.317 microns [ $\beta = 4.58$  degrees]. Illuminating the reference beams were guided through optical fibers to simplify the optical system.

The analysis consisted of digitizing holo-interferometric images of the unloaded package with only a carrier fringe pattern (Figure 4), and of the loaded package showing the combined carrier and deformation pattern (Figure 5). In service, the hermetically sealed package and its internal components are subjected to thermal cycling which causes internal pressure changes. For this experiment, the package was mounted on a rotation stage to allow generation of the carrier pattern, and fitted with an air valve so that surface deformations could be produced by elevating the internal pressure. Using a thermoplastic holocamera a hologram was made of the package, and then the package was rotated 0.0114 degrees about a vertical axis so that the left side of the package moved toward the observer. A photograph was then taken of the real-time fringe pattern caused by interference between the wavefront from the holographic image of the package and the wavefront from the actual package. The internal pressure of the package was elevated and another photograph of the real-time fringe distribution was taken. These are given in Figures 4 and 5. A simple holo-interferogram of the same deformation field is shown in Figure 6 for reference purposes.

The fringe patterns obtained from the two photographs shown in Figures 4 and 5 were smoothed and filtered. Phase shifts were determined by locating the extrema of the intensity distribution plots. Figure 7 shows the phase shift introduced by the carrier, and that caused by the superposition of the deformation on the carrier, obtained by scanning a horizontal line across the center of the package. Here the  $x$  axis originates at the center of the package and the width of the package is given as  $w$ . As illustrated in Figure 8, the subtraction of the curves in Figure 7 gives the fringe order plot required to calculate the magnitude and direction of the surface deflection due to the pressure variation. Results indicate that the fringes shown in Figure 6 correspond to motion toward the observer.

The application of this process to obtain deflection across the entire specimen required some intervention on the part of the investigator. In studying the disk, fringe orders could be readily established knowing that the outer boundary remained stationary. In the present case, however, some fringes run off the edge of the field of view (especially when the carrier is modulated as shown in Figure 5) and the computer is unable to establish the proper sequence for numbering them. In addition, the raised portion of the package along its edges creates an abrupt change in intensity. This was mistakenly recorded as a fringe order in several of the automated scans.



## REFERENCES

Finally, Figures 9 and 10 show the carrier and modulated carrier for a printed wiring board with five symmetrically arrayed leadless ceramic chip carriers. The test module was mounted vertically by clamping along the two sides of the printed wiring board, and thermally loaded by powering the central chip carrier.

Efforts to automatically measure deformation over the entire surface of the board proved more difficult than anticipated. The irregular surface contours and mounting hardware, coupled with abrupt fluctuations in intensity, could be controlled only with significant user interaction, and the automated whole-field approach had to be modified.

A rectangular window (extracted from the data file by numerical algorithms) was used to isolate only the central chip carrier along with the two carrier fringe patterns recorded in that area. Figure 11 shows the result of automated analysis by scanning along a horizontal line through the center of that region. The general shape and magnitude of the deflection seems reasonable when compared to the conventional holo-interferometric fringe pattern shown in Figure 12 for reference purposes. This conventional holo-interferometric fringe pattern represents a contour mapping of the entire out-of-plane deflection field at a sensitivity of around  $0.31 \mu\text{m}/\text{fringe}$ . It should be noted that much less information can be extracted from visual inspection of this type of fringe pattern in the neighborhood of the central chip assembly than was obtained by analysis of the carrier fringe patterns described above.

## Conclusion

A method for automating measurements of complex deformations has been studied. The method has potential but there are still many problems to resolve. In the three samples cited above, excellent results were obtained from the disk where the specimen had fixed boundary conditions and a flat surface with relatively uniform reflectivity. Abrupt changes in intensity and the problem of fringes disappearing over the edge of the specimen posed some problems in the case of the hermetically sealed microelectronic package but these were overcome with some user intervention. The third case involving complex deformations in printed wiring boards with surface mounted components proved intractable to automated whole field analysis using the existing routines. A "windowing" approach has been suggested to circumvent these difficulties by isolating and analyzing selected sub-regions of the displacement field, but even semi-automating this approach will require further refinement of the numerical algorithms.

## Acknowledgement

The authors wish to acknowledge the support of AT&T Bell Laboratories, Marquette University, and the University of Alabama in Huntsville. Since 1980, Professor Gilbert's efforts in holography have been supported in part by contracts DAAG 29-84-K-0183, DAAG 29-84-G-0045, and DAAL 03-86-K-0014 with the Army Research Office in Research Triangle Park, N.C.

- [1] Lanzl, F., Schluter M., Microprocessor-controlled hologram analysis, IEEE 5th International Computing Conference, London, 159-162 (1978).
- [2] Hot, J. P., Durou, C., System for the automatic analysis of interferograms obtained by holographic interferometry, SPIE 2nd European Congress on Optics Applied to Metrology 210, 144-151, (1979).
- [3] Lamy, F., Liegeois, C., Meyrueis, P., Automatic computer analysis of double exposure holograms in industrial nondestructive control, Proceedings of the SPIE 353, 82-89, (1983).
- [4] Katzir, Y., Friesem, A. A., Glaser, I., Sharon, B., Holographic nondestructive evaluation with on line acquisition and processing, Industrial and Commercial Applications of Holography, Milton Chang, Editor, Proc. SPIE 353, 74-81 (1982).
- [5] Sciammarella, C. A., Ahmadshahi, M., Computer based method for fringe pattern analysis, Proc. of the 1984 SEM Fall Conference, Milwaukee, WI, 61-69, (1984).
- [6] Plotkowski, P. D., Hung, Y. Y., Hovanesian, J. D., Gerhart, G., Improved fringe carrier technique for unambiguous determination of holographically recorded displacements, Opt. Eng., 24, 754-756, (1985).
- [7] Matthys, D. R., Dudderar, T. D., Gilbert, J. A., Automated analysis of holo-interferograms for determination of surface displacements, submitted for publication (1985).
- [8] Gilbert, J. A., Dudderar, T. D., Schultz, M. E., Boehnlein, A. J., The monomode fiber-a new tool for holographic interferometry, Exp. Mech. 23, 190-195, (1983).
- [9] Dudderar, T. D., Gilbert, J. A., Real-time holographic interferometry through fiber optics, J. Phys. E: Sci. Instrum. 18, 39-43, (1985).
- [10] Hung, Y. Y., Taylor, C. E., Measurement of surface displacements normal to the line of sight by holo-moire interferometry, J. Appl. Mech., 42, 1-4, (1975).
- [11] Sciammarella, C. A., Gilbert, J. A., A holographic-moire technique to obtain separate patterns for components of displacement, Exp. Mech., 16, 215-220, (1976).
- [12] Hall, P. M., Dudderar, T. D., Argyle, J. F., Thermal deformation observed in leadless ceramic chip carriers surface mounted to printed wiring boards, IEEE Trans., Components, Hybrids and Manufacturing Technology, Vol. CHMT-6, 544-552, (1983).
- [13] Dudderar, T. D., Hall, P. M., Gilbert, J. A., Holo-interferometric measurement of the thermal deformation response to power dissipation in multilayer printed wiring boards, Exp. Mech., 25, 95-104, (1985).
- [14] Dudderar, T. D., Hall, P. M., Gilbert, J. A., Holo-interferometric studies of thermal deformations in microelectronic modules, Proceedings of the 1985 SEM Spring Conference on Exp. Mech. Las Vegas, Nevada, 303-308, (1985).
- [15] Dudderar, T. D., Gilbert, J. A., Hall, P. M., Matthys, D. R., Whole field deformation in printed wiring boards, Proceedings of the 1985 SEM Fall Meeting on Experimental Mechanics, Grenelefe, Florida, 28-35, (1985).



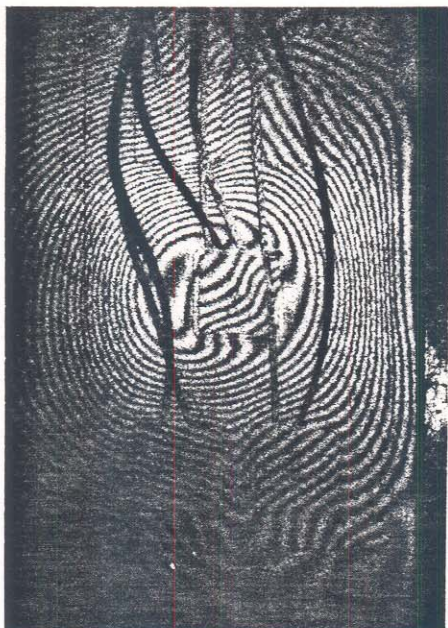


Figure 1. A printed wiring board with five powered, surface mounted ceramic chip carriers and the associated holographic interference fringe pattern.

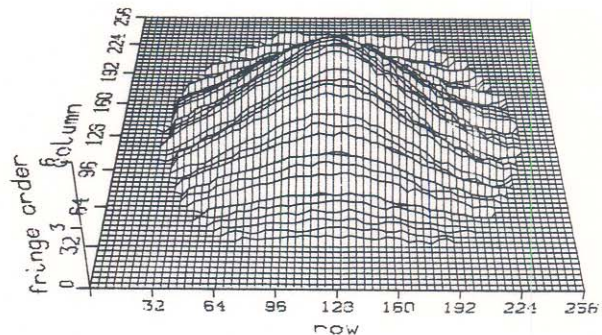
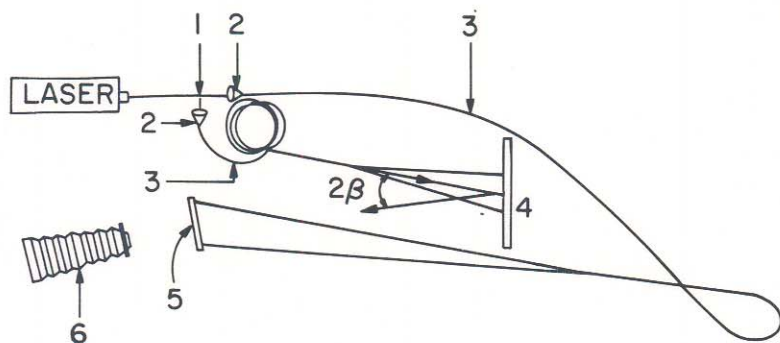


Figure 2. An isometric plot of the deflection of a centrally loaded disk clamped around its boundary, obtained by fully automated analysis.



- 1 - VARIABLE BEAM SPLICER
- 2 - FIBER LAUNCH OPTICS
- 3 - SINGLE MODE OPTICAL FIBER
- 4 - MODEL
- 5 - HOLOGRAM PLATE
- 6 - CAMERA SYSTEM

Figure 3. A real-time holographic/fiber optic recording system.

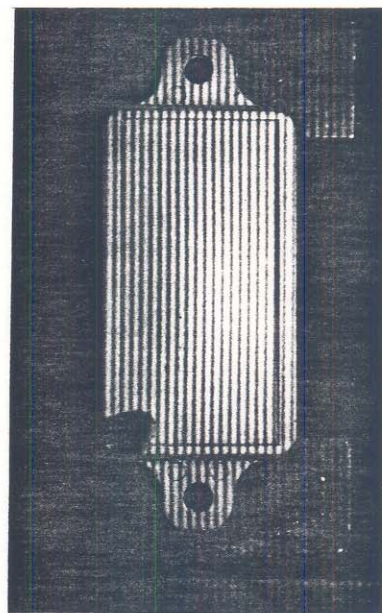


Figure 4. A hermetically sealed microelectronic package with a holo-interferometric carrier fringe pattern.

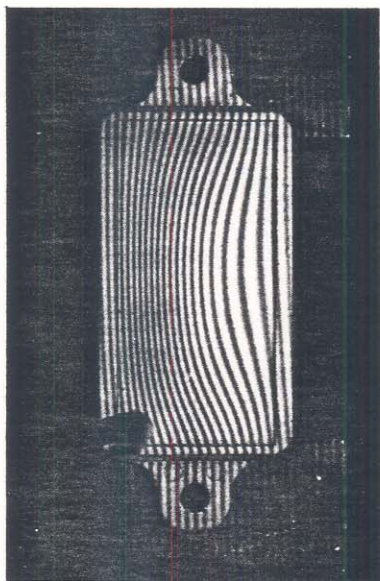


Figure 5. A hermetically sealed microelectronic package showing a carrier fringe pattern modulated by the deflections caused by a change in internal pressure.

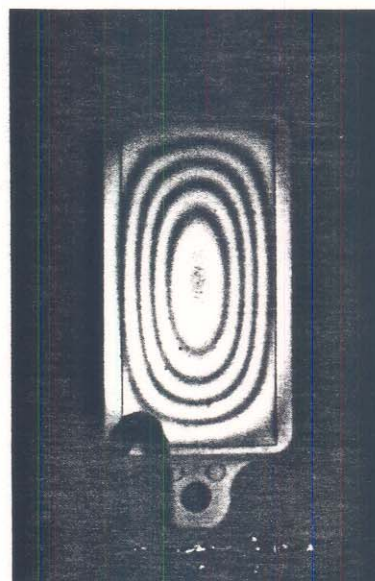


Figure 6. Deflection fringe pattern recorded on the surface of the same microelectronic package caused by a change in internal pressure.

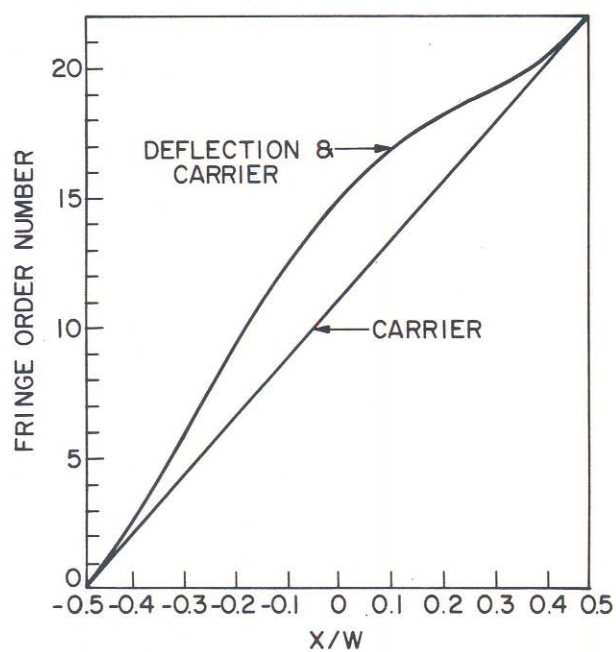


Figure 7. Phase distributions (fringe order plots) of the carrier, and carrier plus deformation along the center of the hermetically sealed microelectronic package.

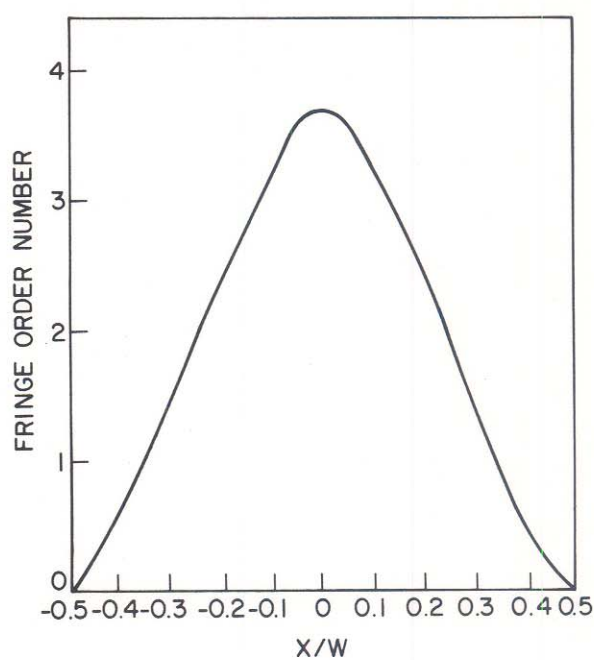


Figure 8. Fringe order plot corresponding to the deflection along the center of the hermetically sealed microelectronic package.



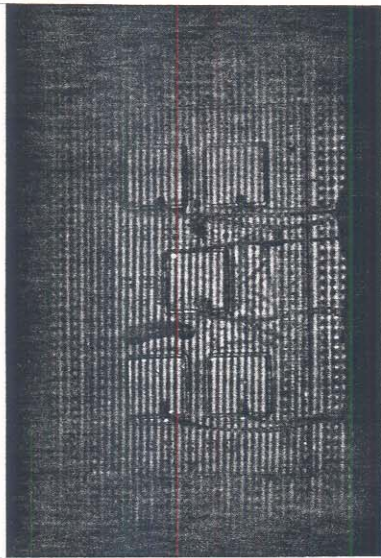


Figure 9. A printed wiring board with a holo-interferometric carrier fringe pattern.

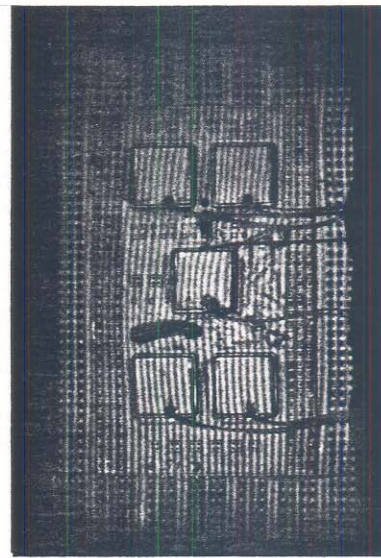


Figure 10. A printed wiring board showing a carrier fringe pattern modulated by the deflection field due to thermal loading.

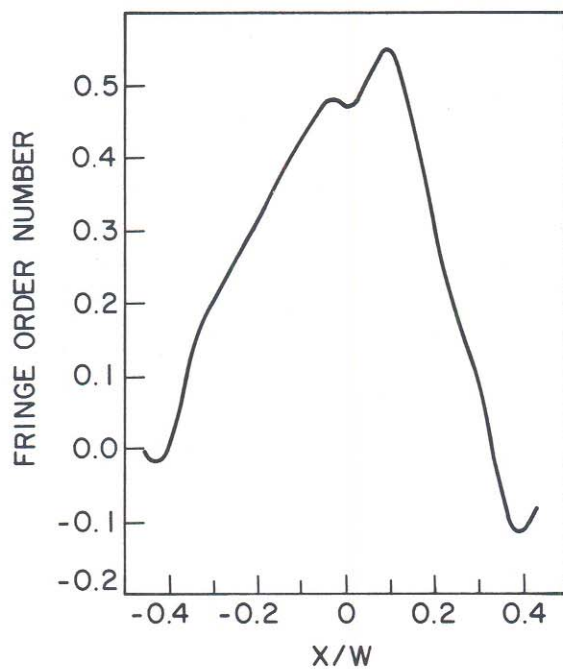


Figure 11. Fringe order plot corresponding to the deflection along the center line of the central ceramic chip carrier on a printed wiring board (see Figure 9, 10 and 12).



Figure 12. Deflection fringe pattern on the surface of the printed wiring board caused by thermal loading.